

Analysis and Reduction of Cogging Torque of Line-Start Permanent Magnet Motors

Libing Jing^{*}, Jun Gong, and Ying Lin

Abstract—Compared with a standard permanent magnet synchronous motor, a line-start permanent magnet synchronous motor (LSPMSM) has additional features that include two-sided slots on its stator and rotor. Thus, due to its complex air gap form, there is no simple method to calculate the cogging torque of this kind of motor at present. This paper presents a new analytical method that models the rotor as an equivalent magnetic motive force (MMF) distribution in the air gap which avoids the influence of rotor slotting in the air gap. Based on the energy method, an analytical method is presented here to analyze the pole-slot match of stator and the influence of number of slots per pole of rotor on the cogging torque. The effect of auxiliary slots on cogging torque of LSPMSM is studied, and by changing the number of auxiliary slots to reduce the cogging torque, the correctness of the above method has been validated by the finite element method.

1. INTRODUCTION

Recently, the performances of permanent magnet (PM) materials have been highly improved, and their price is decreasing. Thus, permanent magnet synchronous motors (PMSM) are gradually used in many industrial applications for their high power factor, high power density, and efficiency. The line start permanent magnet synchronous motors (LSPMSM) have been identified as one of the very promising topologies for line started electric drives designated for energy saving in many applications [1–5]. The main application of LSPMSM is a low cost electric drive without voltage-source inverters [6–9].

Torque ripple is an important parameter of PMSM. How to reduce torque ripple is the key to study the LSPMSM. Different methods are proposed to improve the starting and steady state performance of LSPMSM. Reference [10] present a synchronization capability of LSPMSM with small saliency ratio and high cage resistance, which has beneficial effects on the early start and has a large value of the slip. The starting torque and synchronization capability of LSPMSM are improved in [11], and pole changing at start up neutralizes the magnetic influence of PM, which leads to the elimination of braking and torque ripple and enhances the starting torque. The starting performance of the LSPMSM is studied with different rotor bar design in [12]. In order to solve the aforementioned problems, an analytical dynamic electromechanical model using layer theory is proposed in [13].

The air gap shape is complex for an LSPMSM with two-sided slots which makes it difficult to perform its cogging torque analysis. Moreover, it also makes it difficult to use the cogging torque analysis method for PM with one-sided slots [14–19]. Reference [20] divides the air gap of LSPMSM into stator side and rotor side. Considering the relative position angle between them, the expression for the effective length of air gap is derived by superposition. Then the analytical expression for the cogging torque is derived based on the energy method, and the mechanism of production of the cogging torque is analyzed. However, the complexity of the effective air gap length expression results in a complex expression of the cogging torque. Due to this, further work on cogging torque becomes difficult.

Received 9 December 2018, Accepted 18 January 2019, Scheduled 28 January 2019

^{*} Corresponding author: Libing Jing (jinglibing163@163.com).

The authors are with the College of Electrical Engineering & New Energy, China Three Gorges University, Yichang 443002, China.

This paper presents a new analytical method to analyze the cogging torque of LSPMSM, representing the rotor as an equivalent air gap MMF distribution. In this way, the effective air gap length is only related to the stator, avoiding the difficulty in calculating the effective length of air gap that needs to include rotor slotting. Thereafter, the influence of slot-pole combinations and stator slot skew on cogging torque are analyzed, and the validity of the analysis is verified by FEM.

2. ANALYTICAL METHOD FOR COGGING TORQUE

W-shape permanent magnet arrangement has been widely used in LSPMSM. Therefore, this paper uses this structure to analyze the cogging torque of LSPMSM, as shown in Fig. 1. *ANSYS Maxwell* is a premier electromagnetic field simulation software for designing and analyzing electromagnetic and electromechanical devices, which is used for computing the cogging torque. The proposed model is a 10 kW LSPMSM with 6 poles, and the numbers of stator and rotor slots are 36 and 42, respectively.

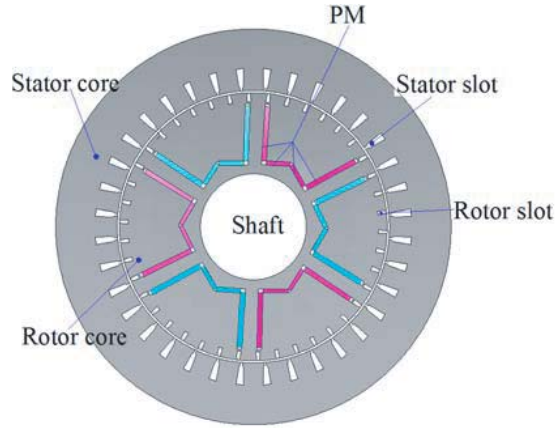


Figure 1. LSPMSM with W-type magnetic circuit.

In order to derive the analytical expression of cogging torque, assume that: 1) the permeability of stator and rotor iron core is infinite; 2) stator and rotor slots are rectangular; 3) the position of $\theta = 0$ is in the centerline of a specific permanent magnet pole; 4) α is the relative position between stator and rotor. When motor rotates, the magnetic field energy in air gap changes because of the changing of air gap permeance causing a change in its torque. The cogging torque T_{cog} is defined as:

$$T_{cog} = -\frac{\partial W(\alpha)}{\partial \alpha} \approx -\frac{\partial W_{airgap}(\alpha)}{\partial \alpha} \quad (1)$$

where W is the magnetic field energy in motor; W_{airgap} is the magnetic field energy in air gap of motor.

Because iron is assumed to have infinite permeability, and its magnetic energy content is negligible,

$$W(\alpha) = W_{airgap}(\alpha) = \frac{1}{2\mu_0} \int_v B^2(\theta, \alpha) dV \quad (2)$$

where μ_0 is the air permeability; $B(\theta, \alpha)$ is the air gap flux density.

Assuming that the inner surface of stator is a magnetic equipotential surface, and the rotor is represented as a distributed magnetic motive force (MMF), the distribution of MMF along air gap is shown as Fig. 2.

This distribution of rotor MMF has considered the influence of rotor slots. Therefore, $B(\theta, \alpha)$ can be expressed as:

$$B(\theta, \alpha) = \Lambda \cdot F(\theta) \quad (3)$$

Among which, Λ is the air permeance per unit area, and $F(\theta)$ is the rotor equivalent MMF. This paper is not for the precise calculation of cogging torque. So a specific value of F is not given. Then, Λ can

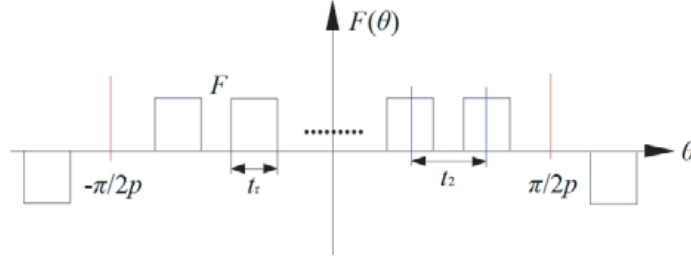


Figure 2. The distribution of rotor's Equivalent MMF.

be expressed as:

$$\Lambda = \frac{\mu_0}{\delta(\theta, \alpha)} \quad (4)$$

where $\delta(\theta, \alpha)$, as the effective distribution of air gap length along the circumference, is related only to the distribution of stator slots. Here, using the cogging torque analysis for one-sided slots can now be applied [21]. Plugging formulas (3) and (4) into formula (2), we get:

$$W_{airgap}(\alpha) = \frac{\mu_0}{2} \int_V F^2(\theta) \left[\frac{1}{\delta(\theta, \alpha)} \right]^2 dV \quad (5)$$

If the Fourier expansion of $F^2(\theta)$ and $[1/\delta(\theta, \alpha)]^2$ can be derived, the expression of magnetic energy of the motor and subsequently the expression of cogging torque can be obtained.

2.1. Fourier Expansion of $F^2(\theta)$

In a permanent magnet machine with uniform distribution of magnets, the distribution of effective MMF, $F(\theta)$, along the air gap is shown in Fig. 2. The Fourier expansion of $F^2(\theta)$ in the interval between $-\pi/2p$ and $\pi/2p$ can be obtained:

$$F^2(\theta) = F_0 + \sum_{n=1}^{\infty} F_n \cos 2np\theta \quad (6)$$

where the Fourier coefficient is:

$$F_0 = \frac{(q_2 - 1)pF^2}{\pi} t_r \quad (7)$$

$$F_n = \begin{cases} (-1)^{n+1} \frac{2F^2}{n\pi} \sin npt_r, & n \text{ is not the integral multiple of } q_2 \\ (-1)^n \frac{2(q_2 - 1)F^2}{n\pi} \sin npt_r, & n \text{ is the integral multiple of } q_2 \end{cases} \quad (8)$$

where the rotor's number of slots per pole is $q_2 = Q_2/2p$; p is the number of pole-pairs; Q_2 is the number of rotor slots; t_r is the tooth width of rotor; and F is the amplitude of air gap MMF.

2.2. Fourier Expansion of $[1/\delta(\theta, \alpha)]^2$

The calculation method of air gap effective length for the permanent magnet motor with one-sided slots is used for reference. When performing the Fourier decomposition for $[1/\delta(\theta, \alpha)]^2$, do not consider the influence of relative position of stator and rotor initially. Assume that the centerline of the tooth is located at $\theta = 0$, and the Fourier expansion of $[1/\delta(\theta, \alpha)]^2$ is:

$$\left[\frac{1}{\delta(\theta, \alpha)} \right]^2 = G_0 + \sum_{n=1}^{\infty} G_n \cos nQ_1(\theta + \alpha) \quad (9)$$

where the Fourier coefficients are given as:

$$G_0 = \frac{Q_1 t_s}{2\pi\delta^2} \quad (10)$$

$$G_n = \frac{2}{n\pi\delta^2} \sin\left(n\pi - \frac{nQ_1 t_s}{2}\right) \quad (11)$$

where Q_1 is the number of stator slots, t_s the tooth width, and δ the actual air gap length.

2.3. The Cogging Torque Expression without Considering the Skewed Slots of Stator

When $m \neq n$, the integral of trigonometric function within $[0, 2\pi]$ satisfies:

$$\begin{cases} \int_0^{2\pi} \cos m\theta \cos n\theta = 0 \\ \int_0^{2\pi} \sin m\theta \cos n\theta = 0 \\ \int_0^{2\pi} \sin m\theta \sin n\theta = 0 \end{cases} \quad (12)$$

Plugging formulas (5), (6) and (10) into formula (1), and making use of formulas of (12), the cogging torque expression of LSPMSM without considering stator skewed slots is:

$$T_{\text{Cog}} = \frac{\pi\mu_0 Q_1 L_a}{4} (R_1^2 - R_2^2) \sum_{n=1}^{\infty} n G_n F_{\frac{nQ_1}{2p}} \sin(nQ_1\alpha) \quad (13)$$

where L_a is the axial length of motor; R_1 and R_2 are the stator inner radius and rotor outer radius, respectively; n is the harmonic order.

3. THE INFLUENCE OF SLOT-POLE MATCH ON COGGING TORQUE

3.1. Slot-Pole Match of Stator

Within the scope of a pitch that the relative positions of stator and rotor change, the cogging torque changes periodically. Changing cycles depend on the slot-pole match. It can be seen from the expression of cogging torque that harmonic number N_p is the minimum value of integer n which makes $nQ_1/2p$ an

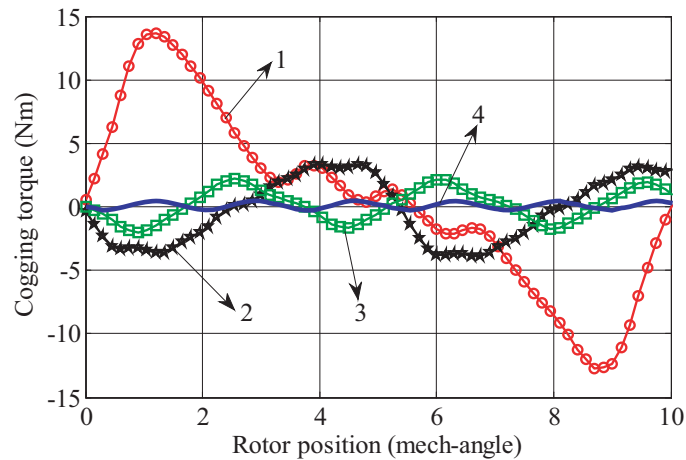


Figure 3. Cogging torque waveform with different stator slot-pole matches.

integer. Therefore, the harmonic number N_p is the ratio of the number of poles to the greatest common divisor between slot number and pole number:

$$N_p = \frac{2p}{GCD(Q_1, 2p)} \quad (14)$$

where $GCD(Q_1, 2p)$ is the greatest common divisor between stator slot number and pole number. It can be seen that the stator slot-pole match has an effect on the harmonic number, N_p , of the cogging torque.

In this paper, a 10 kW LSPMSM with 6 poles is used as an example to study the influence of pole-slot match on its cogging torque. Its structure is shown in Fig. 1, and the main parameters are shown in Table 1. Fig. 3 shows the cogging torque waveform of different stator slot-pole matches. The corresponding relation between waveform and slot-pole matches is shown in Table 2.

Table 1. Main parameters of the first prototype motor.

Parameters	Values
Power rating/kW	10
Pole pairs	3
Stator/Rotor slots number	36/42
Stator outer diameter/mm	400
Stator inner diameter /mm	240
Rotor outer diameter/mm	238
Rotor inner diameter/mm	90
Axial length/mm	120
Air gap length/mm	1
Remanence/T	1
Coercivity/(kA/m)	890

Table 2. Corresponding relation between waveform and stator slot-pole matches.

Waveform	Q_1	$2p$	N_p	T_{cog} amplitude (Nm)
1	36	6	1	13.64
2	27	6	2	3.45
3	34	6	3	2.13
4	35	6	6	0.43

It can be seen from Fig. 3 and Table 2 that the higher the harmonic order is, the smaller the cogging torque amplitude is. Therefore, choosing an appropriate stator slot-pole match can produce higher harmonics of cogging torque with smaller amplitudes.

3.2. The Influence of Rotor Slot Number on Cogging Torque

By formula (8), the space harmonic order of rotor teeth mainly depends on q_2 , and its harmonic amplitude depends on the width of a rotor tooth and the harmonic order for a given number of rotor poles. When rotor tooth number changes, it does not affect the harmonic order of $F^2(\theta)$ of the cogging torque but does affect the corresponding harmonic order, and then influences the amplitude of the cogging torque.

It can be seen from Fig. 1 that the number of rotor slots is an integral multiple of the pole number, which means that the slot number per pole of rotor q_2 is an integer. If the number of rotor slots per

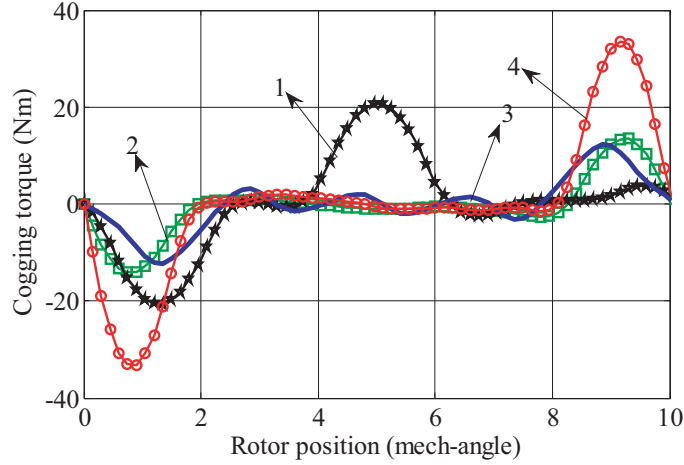


Figure 4. Cogging torque waveform with q_2 .

Table 3. Corresponding relation between waveform with q_2 .

Waveform	q_2	T_{cog} amplitude (Nm)
1	3	20.63
2	4	13.41
3	5	12.22
4	6	33.57

pole is not an integer, it may cause serious flux leakage. Therefore, in this paper, the analysis of cogging torque in LSPMSM is only limited to the integral number of rotor slots per pole. FEM is used for calculating the cogging torque waveform with different q_2 , shown in Fig. 4. The corresponding relation between waveform and q_2 is given in Table 3.

It can be seen from Fig. 5 and Table 4 that the cogging torque amplitude varies considerably with q_2 . For prototype one, the generated cogging torque is the F_{6n} th harmonic of $F^2(\theta)$. When $q_2 = 5$, the F_{6n} th harmonic of $F^2(\theta)$ generated by rotor tooth harmonic is less, so the amplitude of cogging torque is low. When motor is running, N_{q_2} and its multiple times harmonic in $F^2(\theta)$ are influenced by rotor slots. The order of corresponding rotor tooth harmonic is N_{q_2}/q_2 and its multiples:

$$N_{q_2} = LCM \left(\frac{N_p Q_1}{2p}, q_2 \right) \quad (15)$$

where LCM is the least common multiple.

Table 4 compares the corresponding N_{q_2}/q_2 and N_{q_2} with different q_2 . It can be seen that:

- When $q_2 = 3$, $q_2 = 4$, $q_2 = 5$, $q_2 = 6$, N_{q_2}/q_2 are respectively 2, 3, 6 and 1. When $q_2 = 6$, the cogging torque is the largest, and $q_2 = 3$ takes the second place. When $q_2 = 4$ and $q_2 = 5$, the cogging torque is minimum. Therefore, when N_{q_2}/q_2 is larger, the generated cogging torque amplitude is smaller. Because when N_{q_2}/q_2 is larger, the rotor harmonic order is higher and the amplitude smaller, the generated cogging torque is smaller.
- When $q_2 = 3$ or $q_2 = 6$, N_{q_2} is always 6; when $q_2 = 4$ or $q_2 = 5$, N_{q_2} are respectively 12 and 30. Therefore, when N_{q_2} is larger, the generated cogging torque amplitude is smaller. According to the analytical expression of cogging torque, the n th harmonic amplitude of cogging torque is related to the $nQ_1/2p$ th harmonic of $F^2(\theta)$ and n th harmonic amplitude of $[1/\delta(\theta, \alpha)]^2$. When N_{q_2} is larger, the harmonic order of $F^2(\theta)$ influenced by rotor slots is higher, and the corresponding harmonic order of $[1/\delta(\theta, \alpha)]^2$ is also higher, and its amplitude is smaller, which leads to a smaller cogging torque.

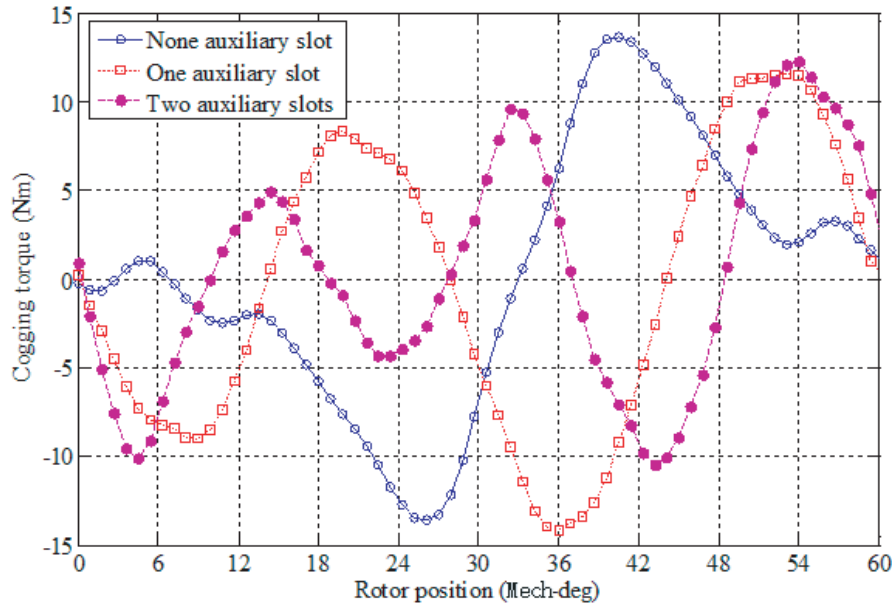


Figure 5. Cogging torque waveform with different auxiliary slots number.

Table 4. Comparisons between N_{q2}/q_2 and N_{q2} with different q_2 .

q_2	N_{q2}/q_2	N_{q2}
3	2	6
4	3	12
5	6	30
6	1	6

Therefore, choosing an appropriate number of rotor slots to increase N_{q2}/q_2 and N_{q2} may get smaller cogging torque.

4. MEASURE TO DECREASE COGGING TORQUE

When auxiliary slots are introduced, they are evenly distributed on armature teeth. Auxiliary slot width is the same as the armature slot-opening width. The depth of auxiliary slots should be appropriate. The effect may not be obvious if it is too shallow and may affect the magnetic circuit of teeth if it is too deep. The key point is whether the influences of auxiliary slot and normal armature slot on air gap magnetic field are same or not, which can be ensured by observing the radial component distribution of air gap flux density calculated by FEM. Introduce k auxiliary slots on each stator tooth.

When the number of auxiliary slots is even, the Fourier decomposition coefficient of $[1/\delta(\theta, \alpha)]^2$ is:

$$\begin{aligned}
 G_n &= \frac{2}{n\pi\delta^2} \left[\sin\left(n\pi - \frac{nQ_1t_s}{2}\right) - 2 \sin \frac{nQ_1t_s}{2} \sum_{i=1,3,5,\dots}^{k-1} \cos \frac{in\pi}{k+1} \right] \\
 &= \begin{cases} \frac{2}{n\pi\delta^2}(k+1) \sin\left(n\pi - \frac{nQ_1t_s}{2}\right), & n \text{ is the multiple of } (k+1) \\ \frac{2}{n\pi\delta^2} \left[\sin\left(n\pi - \frac{nQ_1t_s}{2}\right) + \sin \frac{nQ_1t_s}{2} \cos(n\pi) \right] = 0, & n \text{ is not the multiple of } (k+1) \end{cases} \quad (16)
 \end{aligned}$$

When the number of auxiliary slots is odd, the Fourier decomposition coefficient of $[1/\delta(\theta, \alpha)]^2$ is:

$$G_n = \frac{2}{n\pi\delta^2} \left[2 \cos \frac{n\pi}{2} \sin\left(\frac{n\pi}{2} - \frac{nQ_1 t_s}{2}\right) - 2 \sin \frac{nQ_1 t_s}{2} \sum_{i=1,3,5,\dots}^{\frac{k-1}{2}} \cos \frac{in\pi}{k+1} \right]$$

$$= \begin{cases} -\frac{2}{n\pi\delta^2}(k+1) \sin \frac{nQ_1 t_s}{2}, & n \text{ is the multiple of } (k+1) \\ \frac{2}{n\pi\delta^2} \left[\sin\left(n\pi - \frac{nQ_1 t_s}{2}\right) + \sin \frac{nQ_1 t_s}{2} \cos(n\pi) \right] = 0, & n \text{ is not the multiple of } (k+1) \end{cases} \quad (17)$$

By comparing formulas (11), (16) and (17), it can be seen that when introducing k auxiliary slots on each tooth, G_n is not zero, and only when n is the multiple of $(k+1)$, the value of G_n (not zero) will be the multiple of $(k+1)$ of G_n . Because of the same interval, the expressions of cogging torque with or without auxiliary slots both are formula (13).

According to the previous analysis, to weaken the cogging torque, the number of auxiliary slots must satisfy $(k+1) \neq mN_p$. When $N_p = 1$, whatever the value of k is, the condition of $(k+1) \neq mN_p$ cannot be satisfied. Therefore, the method of introducing auxiliary slots cannot weaken cogging torque. Take prototype one as an example. $N_p = 1$, and whatever the k is, G_{k+1} always influences the cogging torque. Fig. 5 shows the comparison of cogging torque with different auxiliary slots. It can be seen that introducing auxiliary slots will not reduce cogging torque.

When $N_p \neq 1$, the number of auxiliary slots, k , needs to meet $(k+1) \neq mN_p$ (m is integer) to ensure that there is no effect of amplified G_{k+1} on cogging torque. Take a PM motor with 6 poles and 33 slots as an example. $N_p = 2$, and when n is the multiple of 2, G_n will have influence on cogging torque. To reduce cogging torque, it must be ensured that G_{k+1} will have no effect on cogging torque. The comparison of cogging torque without or with one, two or three auxiliary slots is shown in Fig. 6. It can be seen that when the number of auxiliary slots is 2, the cogging torque is greatly weakened, because G_3 is amplified. However, G_3 has no effect on cogging torque. In fact, G_2 and G_4 can influence cogging torque, but these two are greatly weakened. The low order harmonics are weakened, so the cogging torque is reduced. When the number of auxiliary slots is one or three, G_2 and G_4 are amplified. Both of them have effect on cogging torque, so the cogging torque is not reduced but increased.

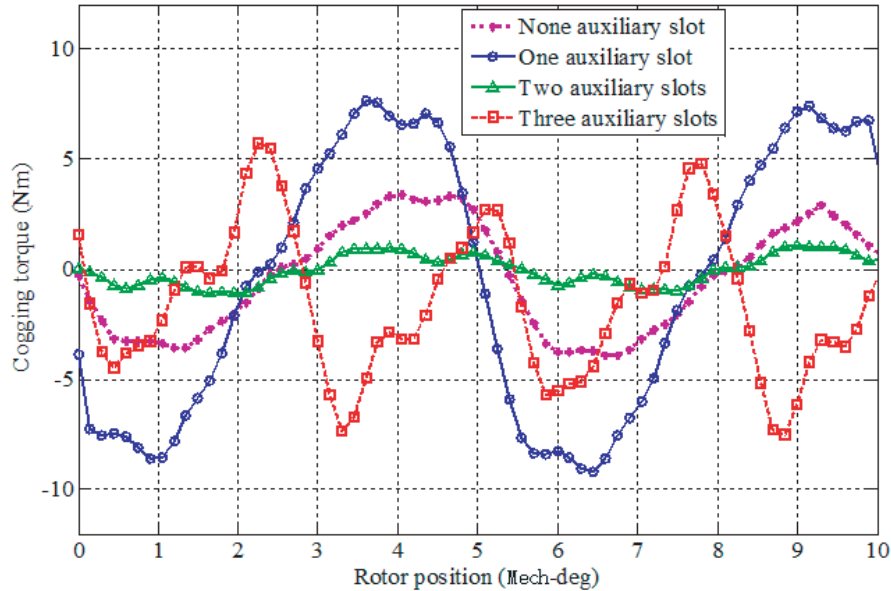


Figure 6. Cogging torque waveform with different auxiliary slots number.

To sum up, the choice principles of number of auxiliary slots, k , are as follows:

(1) When $N_p = 1$, no matter what the number of auxiliary slots is, G_{k+1} will affect the cogging torque.

(2) When $N_p \neq 1$, if the number of auxiliary slots k satisfies $(k + 1) \neq mN_p$, the selected number of auxiliary slots ensures that G_{k+1} does not affect the cogging torque.

5. CONCLUSION

This paper presents a new method to analyze the cogging torque of an LSPMSM. The rotor can be represented equivalent to an MMF distribution, and the expressions of cogging torque with or without considering stator skewed slots are deduced based on the energy method. The influence of pole-slot match on cogging torque is analyzed, and the effects of number of stator slots and the number of slots per rotor pole on cogging torque are expounded. Additionally, the influence of auxiliary slots on cogging torque is studied, and it is shown that the cogging torque can be weakened by changing the number of auxiliary slots.

ACKNOWLEDGMENT

This work was supported by the National Natural Science Foundation of China (Project No. 51707072) and China Postdoctoral Science Foundation (Project No. 2018M632855).

REFERENCES

1. Akeshi, T., K. Satoshi, M. Kenji, and B. Andreas, "Asynchronous torque of line-starting permanent-magnet synchronous motors," *IEEE Trans. Energy Convers.*, Vol. 30, No. 2, 498–506, 2015.
2. Mahmoudi, A., S. Kahourzade, N. A. Rahim, H. W. Ping, and N. F. Ershad, "Slot less torus solid rotor ringed line-start axial flux permanent magnet motor," *Progress In Electromagnetics Research*, Vol. 131, 331–355, 2012.
3. Villani, M., M. Santececca, and F. Parasiliti, "High-efficiency line-start synchronous reluctance motor for fan and pump applications," *2018 XIII International Conference on Electrical Machines (ICEM)*, 2178–2184, 2018.
4. Mahmoudi, A., S. Kahourzade, N. A. Rahim, and H. W. Ping, "Improvement to performance of solid-rotor-ringed line-start axial-flux permanent-magnet motor," *Progress In Electromagnetics Research*, Vol. 124, 383–404, 2012.
5. Tian, M. M., X. H. Wang, and D. H. Wang, "The analysis of the influences of switching opportunity for a novel 6/8 pole changing line-start permanent magnet synchronous motor," *20th International Conference on Electrical Machines and Systems (ICEMS)*, 1–5, 2017.
6. Isfahani, A. H. and S. V. Zadeh, "Effects of magnetizing inductance on start-up and synchronization of line-start permanent-magnet synchronous motors," *IEEE Trans. Magn.*, Vol. 47, No. 4, 823–829, 2011.
7. Lee, B. H., J. W. Jung, and J. P. Hong, "An improved analysis method of irreversible demagnetization for a single-phase line-start permanent magnet motor," *IEEE Trans. Magn.*, Vol. 54, No. 11, ID: 8206905, 2018.
8. Aliabad, A. D. and F. Ghoroghchian, "Design and analysis of a two-speed line start synchronous motor: Scheme one," *IEEE Trans. Energy Convers.*, Vol. 31, No. 1, 366–372, 2016.
9. Ugale, R. T. and B. N. Chaudhari, "Rotor configurations for improved starting and synchronous motor," *IEEE Trans. Ind. Electron.*, Vol. 64, No. 1, 138–148, 2017.
10. Stioa, D., K. Hameyer, and B. Drago, "The behavior of the LSPMSM in asynchronous operation," *14th Int. Conf. Power Electronics and Motion Control*, 45–50, 2010.
11. Aliabad, A. D., M. Mojtaba, and F. E. Nima, "Line start permanent magnet motors: significant improvement in starting torque, synchronization, and steady state performance," *IEEE Trans. Magn.*, Vol. 46, No. 12, 4066–4072, 2010.

12. Wei, F. L., Y. L. Luo, and H. S. Zhao, "Influences of rotor bar design on the starting performance of line start permanent magnet asynchronous motor," *6th Int. Conf. Electromagnetic Field Problems and Applications*, 1–4, 2012.
13. Edgar, P. S. and A. C. Smith, "Line start permanent magnet machines using a canned rotor," *IEEE Trans. Ind. Appl.*, Vol. 45, No. 3, 903–910, 2009.
14. Wu, D. and Z. Q. Zhu, "Design tradeoff between cogging torque and torque ripple in fractional slot surface mounted permanent magnet machines," *IEEE Trans. Magn.*, Vol. 51, No. 11, ID: 8108704, 2015.
15. Azar, Z. and Z. Q. Zhu, "Investigation of torque-speed characteristics and cogging torque of fractional-slot IPM brushless AC machines having alternate slot openings," *IEEE Trans. Ind. Appl.*, Vol. 48, No. 3, 903–912, 2012.
16. Ren W., Q. Xu, Q. Li, and L. B. Zhou, "Reduction of cogging torque and torque ripple in interior PM machines with asymmetrical V-type rotor design," *IEEE Trans. Magn.*, Vol. 52, No. 7, ID: 8104105, 2016.
17. Kahourzade, S., A. Mahmoudi, A. Gandomkar, N. A. Rahim, H. W. Ping, and M. N. Uddin, "Design optimization and analysis of AFPMS synchronous machine incorporating power density, thermal analysis, and back-EMF THD," *Progress In Electromagnetics Research*, Vol. 136, 327–367, 2013.
18. Tiang, T. L., D. Ishak, C. P. Lim, and M. R. Mohamed, "Analytical method using virtual PM blocks to represent magnet segmentations in surface-mounted PM synchronous machines," *Progress In Electromagnetics Research B*, Vol. 76, 23–36, 2017.
19. Nguyen, V. T. and T. F. Lu, "Analytical expression of the magnetic field created by a permanent magnet with diametrical magnetization," *Progress In Electromagnetics Research B*, Vol. 87, 163–174, 2018.
20. Wang, X. H., T. T. Ding, and Y. B. Yang, "Study of cogging torque in line-start permanent magnet synchronous motors," *Proceedings of the CSEE*, Vol. 25, No. 18, 167–170, 2005.
21. Kang, G. H., Y. D. Son, and G. T. Kim, "A novel cogging torque reduction method for interior-type permanent magnet motor," *IEEE Trans. Ind. Appl.*, Vol. 45, No. 1, 161–167, 2009.